Radiobiological effects of the interruption time in radiation therapy with photon beams based on the microdosimetric kinetic model

Hisashi Nakano (hisankn@gmail.com)
Osaka University https://orcid.org/0000-0002-9023-880X
Daisuke Kawahara
Hiroshima University
Satoshi Tanabe
Nihon Shika Daigaku Niigata Seimei Shigakubu Daigakuin Niigata Seimei Shigakubu Kenkyuka
Satoru Utsunomiya
Niigata University
Takeshi Takizawa
Niigata University
Hidefumi Aoyama
Hokkaido University

Research

Keywords: External photon beams, Sublethal damage repair, Interruption time, Monte Carlo simulation, Microdosimetric kinetic model

Posted Date: March 19th, 2020

DOI: https://doi.org/10.21203/rs.3.rs-17887/v1

Radiobiological effects of the interruption time in radiation therapy with photon beams based on the microdosimetric kinetic model

Hisashi Nakano[1,*], Daisuke Kawahara[2], Satoshi Tanabe[1],

Satoru Utsunomiya[3], Takeshi Takizawa[4], Hidefumi Aoyama[5]

***Corresponding author:** Hisashi Nakano, Department of Radiation Oncology, Niigata University Medical and Dental Hospital, 1-757 Asahimachi-dori, Chuo-ku, Niigata, Japan.

Tel.: +81-25-227-2315, Fax: +81-25-227-0788

Email: hisankn@gmail.com

Abstract

Background: We investigated the effect of the interruption time on the radiobiological effectiveness with photon beams based on a modified microdosimetric kinetic model.

Background: The interruption time is used is that irradiation interruption occurs at sites and operations such as the gantry, collimator, couch rotation, and patient set-up in radiotherapy. However, the effect of interruption time on photon beams for tumor cells is little evaluated.

Methods: The dose-mean lineal energy y_D (keV/μm) of 6 MV photon beams was calculated by the particle and heavy ion transport system (PHITS). We set the absorbed dose to 2 or 8 Gy, and the interruption time (τ) was set to 1, 3, 5, or 10 min. The biological parameters values were acquired from a human non-small cell lung cancer cell line (NCI-H460) for the mMK model. We used two-field and four-field irradiation with a constant dose rate (3 Gy/min); the photon beams were paused for interruption time τ. We calculated the relative biological effectiveness (RBE) to evaluate the interruption time's effect compared with photon beams that were not interrupted as a reference.

Results: The RBE with four-field irradiation for 8 Gy was decreased to 0.997, 0.992, 0.987, and 0.975 for τ = 1, 3, 5, and 10 min, respectively. The decrease in the RBE was within 3% compared with the non-interrupted photon beams.

Conclusions: The effect of RBE was decreased by increasing the interruption time, indicating that an escalation of the prescribed dose might be necessary when the interruption time was large.

Keywords: External photon beams, Sublethal damage repair, Interruption time, Monte Carlo simulation, Microdosimetric kinetic model

Background

When cells are irradiated with photon beams, the DNA of the cells is damaged. This DNA damage affects the life and death of the cells. However, even when cells' is damaged, some of the cells have the ability to recover from the damage, in a recovery phenomenon known as sublethal damage repair (SLDR) [1, 2]. SLDR is a rapid phenomenon that begins within several minutes and is complete within 4–6 hr after the irradiation of DNA by photon beams [1, 2]. It may therefore be possible to lessen photon beams' effect of cell killing on biological effectiveness by increasing the dose-delivery time, based on SLDR [3, 4]. We have evaluated the effect of the dose-delivery time on biological effectiveness with single-field photon beams based on a microdosimetric kinetic (MK) model [5, 6]; we observed that at 8 Gy irradiation the surviving fraction (SF) was increased by prolonging the dose-delivery time, and the relative biological effectiveness (RBE) was decreased. When the dose-delivery time was 30 min, the decrease was approx. 2%, and in the case of 60 min, the decrease was approx. 6%. However, there was no significant difference of the effect of an approx. 10 min dose-delivery time on the SF of RBE.

Fractionated irradiation with multiple fields has been used in radiation therapy in clinical settings for covering the radiation target with the prescribed dose and preventing toxicity to surrounding normal tissues as much as possible [7]. When multiple-field irradiation is applied, the prescribed dose is not administered consecutively; there is an interruption time, i.e., a certain interval is inserted between each radiation field. The reason why an interruption time is used is that irradiation interruption occurs at sites and operations such as the gantry, collimator, couch rotation, and patient set-up [8, 9]. It is thus necessary to evaluate the effect of multiple-field irradiation to simulate clinical

conditions, since the previous studies evaluated the effect of single-field irradiation on the SF and RBE. In other words, for evaluations of the SF and RBE during irradiation in a single session, it is necessary to set the dose-delivery time while taking the interruption time for each field into account.

Hawkins proposed the MK model based on dual radiation action in 1994 [10, 11] in order to consider the repair-misrepair [12] and lethal and potentially lethal [13] models. The MK model was designed to reveal the relationship between the SF and the absorbed dose (D) by calculating the energy deposition and analyzing the dose-rate effect [10, 11]. Matsuya et al. proposed a modified MK model (mMK model) which considers the various irradiation methods with photon beams [14, 15] and can be used to determin the change of the DNA amount per nucleus during irradiation [16]. This mMK model is able to better estimate the SF with a higher radiation dose range compared to the previous MK model, by taking the cell cycle of cells into consideration. With the mMK model it is also possible to calculate the SF of more clinically relevant conditions due to fractionated irradiation. The effect of the interruption time on the RBE obtained with 6 MV photon beams in multiple-field irradiation has not been evaluated. Furthermore, the effect of the SLDR during the interruption time on the RBE using mMK model, which is a similar method used in previous studies, especially for particle therapy [17-20]. However, there are little studies of photon beams for the effect of interruption time on the RBE. Since photon therapy is more popular than particle therapy, this study may have great impact. We conducted the present study to determine the effects of the interruption time on RBE with the use of photon beams, using the mMK model.

Materials and methods

The MK model

In the MK model, we used the domains in which the nucleus of the considered cell is divided into several hundred independent areas. In the model, potentially lethal lesions (PLLs) occurred after the irradiation of the domains. Based on their transformations, the PLLs are classified into the following four categories. (1) An irreparable lethal lesion (LL) which emerges through a first-order process; the rate constant of the transformation is (a); (2) A PLL converted to an LL through a second-order process; the rate constant of the transformation is (b); (3) A PLL that this repaired through a first-order process; the rate constant of the transformation is (c); and (4) Lesions that resist becoming LLs for a period of time t_r, after which they do become LLs, which are not repairable. The PLLs are thought to be DNA double-stand breaks. According to the original MK model, the average number of LLs per cell nucleus (L_n) is defined as:

$$\begin{aligned} L_n &= N\langle A\langle z\rangle + B\langle z^2\rangle\rangle \\ &= (\alpha_0 + \gamma\beta_0)D + \beta_0 D^2 \\ &= \left(\alpha_0 + \frac{y_D}{\rho\pi r_d^2}\beta_0\right)D + \beta_0 D^2 \\ &= -l_n S \end{aligned} \qquad (1)$$

$$\gamma = \frac{y_D}{\rho\pi r_d^2} \qquad (2)$$

where N is the number of domains, A and B are coefficients, z is the specific energy deposited in the domain [Gy], and the parentheses in the L_n equation indicate the expectation value. The parameter ρ is the density of the domain, and r_d is the radius of the domain (0.5 μm). D is the absorbed dose [Gy], and y_D is the dose-mean lineal energy [keV/μm]. The parameters α_0 and β_0 were obtained by single instantaneous irradiation using the linear-quadratic (LQ) model. The γ value is a coefficient that is calculated by

the dose-mean lineal energy y_D, ρ, π, and r_d (Eq. 2 above).

The modified MK (mMK) model

Matsuya et al. provided the mMK model, considering various irradiation schemes with photon beams [21]. The equation that determines the mMK model is:

$$-l_n S = \sum_{n=1}^{N} [(\alpha_n + \gamma\beta_n) D_n + \beta_0 D_n^2] + 2\sum_{n=1}^{N-1}\sum_{m=n+1}^{N} \{\beta_{nm}[e^{-(m-n)(a+c)\Delta T}]\}(\dot{D}\Delta T)^2 \quad (3)$$

$$\alpha_n = A\langle G_n \rangle \quad (4)$$

$$\beta_n = B\,\langle G_n \rangle^2 \Phi_n \quad (5)$$

$$\beta_{nm} = B\,\langle G_n \rangle \langle G_m \rangle \quad (6)$$

$$D = \dot{D}T \quad (7)$$

$$(a + c) = \frac{ln\,2}{T_{1/2}} \quad (8)$$

where A and B are coefficients, G_n and G_m are the amount of DNA per cell nucleus, Φ_n is a dimensionless parameter, $\dot{D}$ is the dose rate [Gy/min], T is the dose-delivery time [min], and D_n is the absorbed dose at a regular interval [Gy] (Eq. 3). The PLL repair rate of (a + c) equated with the first-order rate λ [21, 22], which was calculated using the DNA repair half-time $T_{1/2}$ [26, 27].

$$-l_n S = \sum_{n=1}^{N} [(\alpha_0 + \gamma\beta_0) D_n + \beta_0 D_n^2] + 2\sum_{n=1}^{N-1}\sum_{m=n+1}^{N} \{\beta_0[e^{-(m-n)(a+c)\tau_n}]\} D_n D_m \quad (9)$$

This equation (Eq. 9) takes into account the interruption of photon beams by using Eq. 3. The interruption time of each field was defined as τ_n [min], and a diagram of the mMK model taking into consideration the interruption time of photon beams is given in Figure 1. The figure also shows that the deformed Eq. 6 could be considered the [min] [min]interruption time for both the linac pulse interval and each field interval. In this study, we calculated the SF when the interrupted photon beams which have two-field and four-field irradiation.

Monte Carlo simulations calculated by the particle and heavy ion transport code system (PHITS)

Monte Carlo simulations code the particle and heavy ion transport code system (PHITS) and can deal with photons, electrons, positrons, neutrons, and heavy ions [24–28]. In the present study, we used the PHITS version 3.02 with the default setting, and we used the International Atomic Energy Agency (IAEA) phase-space file of the Varian TrueBeam linear accelerator (Varian Medical Systems, Palo Alto, CA) to calculate the dose-mean lineal energy y_D of 6 MV photon beams. The irradiation geometry for the 6 MV photon beams (Fig. 2) was used for the PHITS calculations with the default setting; the SSD was 90 cm, the field size was 20 cm × 20 cm. The measurement point was located at a depth of 10 cm, and the calculation width was 3 cm in the water-equivalent phantom material. The radius of the domain was 0.5 μm. The dose-mean lineal energy y_D [26–29] was calculated as:

$$y = \frac{\varepsilon}{l} \qquad (10)$$

$$y_D = \frac{\int y^2 f(y) dy}{\int y f(y) dy} = \frac{\int y d(y) dy}{\int d(y) dy} \quad (11)$$

where ε is the energy deposited in a domain, l is the mean chord length, y is the lineal energy, f(y) is the probability density of the lineal energy, and d(y) is the dose distribution of the lineal energy.

The energy distributions of the 6 MV photon beams in a domain were calculated with the PHITS. The relations yd(y) distributions and y for the photon beams are shown in Figure 3a. We used the yd(y) distributions used for the calculations of the dose-mean lineal energy y_D, with Eq. (8).

The relationships between the depth of the measured position in the water equivalent phantom and the dose-mean lineal energy y_D for the 6 MV photon beams (b) are illustrated in Figure 3. We noted that there was little effect on the value of y_D by changing the water depth. Therefore, y_D was averaged over the depth range of 10–13 cm. The average and standard deviation values of y_D for photon beams are listed in Table 1. We used the average y_D value obtained by simulating the PHITS for the calculations of the SF and biological effectiveness in the mMK model.

The determination of biological parameters for the mMK model by analyzing NCI-H460 lung cancer cells

We used the biological parameters of the human non-small-cell lung cancer cell line NCI-H460 to determine the parameters of the mMK model. The biological parameters α_0 and β_0 using an LQ model were first reported by King et al. [30]. Each of the DNA repairs occurred at a different rate constant, and the DNA repair rate could be calculated as λ in the mMK model (Eq. 5). The biological parameters for the mMK model

simulations of the NCI-H460 cells are shown in Table 1.

The calculations of the SF and RBE for interrupted 6 MV photon beams using the mMK model

The calculation of the SF and RBE using the mMK model was performed with two-field irradiation in this study. The absorbed dose on the NCI-H460 cells was varied from 2 Gy to 8 Gy. The tumor cells were irradiated using two-field irradiation with the absorbed dose D_1 at the constant dose rate $\dot{D}$ (3 Gy/min). The irradiation was interrupted for a certain time (τ). Next, the absorbed dose D_2 was irradiated at the constant dose rate $\dot{D}$ (3 Gy/min). In the four-field irradiation, the absorbed dose for the tumor cells was D_1 at a constant dose rate, $\dot{D}$ (3 Gy/min). The irradiation was interrupted for a certain time (τ).

Second, the absorbed dose D_2 was irradiated at the constant dose rate $\dot{D}$ (3 Gy/min). The irradiation was interrupted for τ. Third, the absorbed dose D_3 was irradiated at the constant dose rate $\dot{D}$ (3 Gy/min). The irradiation was interrupted for τ. Finally, the absorbed dose D_4 was irradiated at the constant dose rate $\dot{D}$ (3 Gy/min). We divided the absorbed dose into two for the two-field irradiation and divided it into four for the four-field irradiation. The RBE of the interrupted photon beams was defined using the instantaneous irradiation (τ = 0) that no interruption of the photon beams as a reference (Eq. 12) [17, 31]:

$$RBE = \left[\frac{D_{\tau=0}}{D_{\tau}}\right] = \left(\frac{\sqrt{\alpha_{\tau=0}^2 + 4\beta_{\tau=0}S_{\tau=0}} - \alpha_{\tau=0}}{2\beta_{\tau=0}}\right)^{-1} \cdot \left(\frac{\sqrt{\alpha^2 + 4\beta S} - \alpha}{2\beta}\right) \quad (12)$$

Results

The effect of the interruption time on the SF for 6 MV photon beams with two-field and four-field irradiation in the mMK model

Figure 4 illustrates the effect of the interruption time on the SF with the two-field and four-field irradiation. The SF was increased with the increase of the interruption time in both the two- and four-field irradiation. The difference between SFs with four-field irradiation was emphasized when the interruption time was 10 min. The effect of the interruption time was greater as the absorbed dose became higher.

The effect of the interruption time on the RBE with two-field and four-field irradiation in the mMK model

Figure 5 shows the RBE of 6 MV photon beams in the two-field and four-field irradiation for different interruption times. The RBE with two-field irradiation was decreased to 0.998, 0.997, 0.993, 0.990 for interruption times τ = 1, 3, 5, 10 min with 2 Gy, and the RBE was decreased to 0.997, 0.992, 0.985, 0.981 for τ = 1, 3, 5, 10 min with 8 Gy, respectively. The RBE of the four-field irradiation was decreased to 0.998, 0.996, 0.991, 0.987 for interruption times τ = 1, 3, 5, 10 min with 2 Gy, and the RBE was decreased to 0.997, 0.992, 0.987, 0.975 for τ = 1, 3, 5, 10 min with 8 Gy, respectively. The RBE was decreased by prolonging the interruption time, and the decrease of the RBE was approx. 2.5% compared with no interrupted photon beams when the absorbed dose was 8 Gy and the photon beams were irradiated with four fields. In addition, the interruption of the photon beams for several minutes had no significant effect on RBE in this study within 3%.

Discussion

It is possible that the photon beams' cell-killing effect on the biological effectiveness was decreased with the increase of the interruption time due to SLDR. We determined the RBE of the 6 MV photon beams for various interruption times, which were calculated from the SF using the mMK model. There was no significant difference in the effect on the RBE when photon beams with two-field and four-field irradiation were interrupted for approx. 10 min compared with instantaneous irradiation (τ = 0 min). However, an approx. 2.5% reduction of the RBE was observed when the four-field irradiation with 8 Gy was interrupted for 10 min. It may thus be necessary to make the interruption of photon beams as quick as possible, since the RBE was decreased by prolonging the interruption time.

In the clinic, the linear accelerators could be occurred the interruptions of irradiation due to mechanical troubles of linear accelerator [32]. In a linear accelerator setting, irradiation may be interrupted for a long period of time due to mechanical trouble. Figure 6 provides the results of our calculation of the effect of the irradiation interruption times of 1 min, 30 min, and 60 min on the SF **(a)** and RBE **(b)**. The RBE was decreased by approx. 2% at 2 Gy and by ~4% at 8 Gy with the 30-min interruption. The RBE was decreased by ~4% at 2 Gy and ~8% at 8 Gy at the 60-min interruption. When the interruption time exceeded 30 min, there was a large dose difference compared with instantaneous irradiation. Based on this result, we speculate that a prescribed dose taking the interruption time into account is required when a long irradiation interruption (>30 min) occurs.

Additionally, Figure 7 shows that the RBE value was dependent on cell-specific values (a + c) (τ = 1, 10 min). We note that the RBE was affected by the value of (a + c),

and the effect of the interruption time differed by >3% when the interruption time was 10 min and the absorbed dose was 8 Gy. The cell-specific value (a + c) (which is an important factor in the mMK model) indicates the recovery from tumor sublethal damage, depending on the type of tumor cell [33, 34]. It is thus necessary to more accurately evaluate the effect of the interruption time for each type of tumor cells in order to simulate clinical conditions.

We used NCI-H460 cells in the mMK model for calculating the effect of the interruption time in this study. We assessed the effect of the interruption time by using the tumor cell parameters of *in vitro* experiments. The *in vivo* study was necessary to investigate the effect of the interruption time because *in vivo* tumor cells behave somewhat differently compared with *in vitro* tumor cells. It is also necessary to further examine the effect of the interruption time in multiple-field therapy, intensity-modulated radiation therapy (IMRT), and volumetric modulated arc therapy (VMAT), as we simulated only two-and four-field irradiation in this study.

Conclusions

The approx. 10-min interruption of 6 MV photon beams had no significant effect on the biological effectiveness, since the RBE decrease was within 3%. Nevertheless, the effect of RBE for a tumor was decreased by increasing the interruption time. It is thus necessary to make the interruption time as short as possible. When the interruption time is long, it is possible that an escalation of the prescribed dose will be needed.

Abbreviations

SLDR, sublethal damage repair; MK model, microdosimetric kinetic model; SF, surviving fraction; RBE, relative biological effectiveness; mMK model, modified microdosimetric kinetic model; PLL, potentially lethal lesion; LL, lethal lesion; PHITS, particle and heavy ion transport system**;** IAEA, International Atomic Energy Agency; IMRT, intensity-modulated radiation therapy; VMAT, volumetric modulated arc therapy.

Ethical Approval and Consent to participate

Not applicable.

Consent for publication

Not applicable.

Availability of supporting data

Not applicable.

Competing interests

The authors declare that they have no competing interests.

Funding

This work was funded by JSPS KAKENHI Grant Number 19K17227.

Authors' contributions

HN performed the planning study and the statistical analysis, and drafted the manuscript. DK performed the planning study and made the study design. ST, SU, TK and HA conceived of the study, and participated in its design and coordination, and helped to draft the manuscript. All authors read and approved the final manuscript.

Acknowledgements

Not applicable.

Authors' information

[1]Department of Radiation Oncology, Niigata University Medical and Dental Hospital, 1-757 Asahimachi-dori, Chuo-ku, Niigata, Japan

[2]Department of Radiation Oncology, Institute of Biomedical & Health Sciences, 1-2-3 Kasumi, Minami-ku, Hiroshima-shi, Hiroshima, Japan

[3]Department of Radiological Technology, Niigata University Graduate School of Health Sciences, 2-746 Asahimachi-dori, Chuo-ku, Niigata, Japan

[4]Niigata Neurosurgical Hospital, Niigata, 3057 Yamada, Nishi-ku, Niigata, Japan

[5]Department of Radiology and Radiation Oncology, Niigata University Graduate School of Medical and Dental Sciences, 1-757 Asahimachi-dori, Chuo-ku, Niigata, Japan

References

1. Elkind MM, Sutton H. Radiation response of mammalian cells grown in culture. Repair of X-ray damage in surviving Chinese hamster cells. Radiat Res 1960;13:556-593.

2. Elkind MM. Repair processes in radiation biology. Radiat Res 1984;100:425-49.

3. Shibamoto Y, Ito M, Sugie C. Recovery from sublethal damage during intermittent exposures in cultured tumor cells: Implications for dose modification in radiosurgery and IMRT. Int J Radiat Oncol Biol Phys 2004;59:1484-1490.

4. Sugie C, Shibamoto Y, Ito M. Radiobiologic effect of intermittent radiation exposure in murine tumors. Int J Radiat Oncol Biol Phys 2006;64:619-624.

5. Nakano H, Kawahara D, Ono K. Effect of dose-delivery time for flattened and flattening filter-free photon beams based on microdosimetric kinetic model. PLoS One 2018;13:e0206673.

6. Kawahara D, Nakano H, Ozawa S. Relative biological effectiveness study of Lipiodol based on microdosimetric-kinetic model. Phys Med 2018;46:89-95.

7. Frank Pajonk, Erina Vlashi, William H McBride. Radiation resistance of cancer stem cells: The 4 R's of radiobiology revisited. Stem cells 2010;28:639-648.

8. Bai S, Li G, Wang M. Effect of MLC leaf position, collimator rotation angle, and gantry rotation angle errors on intensity-modulated radiotherapy plans for nasopharyngeal carcinoma. Med Dosim 2013;38:143-147.

9. Smyth G, Bamber JC, Evans PM. Trajectory optimization for dynamic couch rotation during volumetric modulated arc radiotherapy. Phys Med Biol 2013;58:8163-8177.

10. Hawkins RB. A statistical theory of cell killing by radiation of varying linear energy transfer. Radiat Res 1994;140:366-374.

11. Hawkins RB. A microdosimetric-kinetic model of cell death from exposure to

ionizing radiation of any LET, with experimental and clinical applications. Int J Radiat Biol 1996;69:739-755.

12. Tobias CA, Blakely EA, Ngo FQH. The repair-misrepair model of cell survival. In: Meyn RE, Withers HR (eds). Radiation Biology in Cancer Research. New York: Raven 1980, 195-230.

13. Curtis SB. Lethal and potentially lethal lesions induced by irradiation a unifed repair model. Radiat Res 1986;106:252-270.

14. Matsuya Y, Ohtsubo Y, Tsutsumi K. Quantitative estimation of DNA damage by photon irradiation based on the microdosimetric-kinetic model. J Radiat Res 2014;55:484-493

15. Matsuya Y, Tsutsumi K, Sasaki K. Evaluation of the cell survival curve under radiation exposure based on the kinetics of lesions in radiation to dose-delivery time. J Radiat Res 2015;56:90-99.

16. Matsuya Y, Tsutsumi K, Sasaki K. Modeling ell survival and change in amount of DNA during protracted radiation. J Radiat Res 2017;58:302-312.

17. Inaniwa T, Kanematsu N, Suzuki M. Effects of beam interruption time on tumor control probability in single-fractionated carbon-ion radiotherapy for non-small cell lung cancer. Phys Med Biol 2015;60(10):4105-4121.

18. Inaniwa T, Suzuki M, Furusawa T. Effects of dose-delivery time structure on biological effectiveness for therapeutic carbon-ion beams evaluated with microdosimetric kinetic model. Radiat Res 2013;180(1):

19. Manganaro L, Russo G, Cirio R. A Monte Carlo approach to the microdosimetric kinetic model to account for dose rate time structure effects in ion beam therapy with application in treatment planning simulations. Med Phys 2017;44(4):1577-1589.

20. Takei H, Inaniwa T. Effect of Irradiation Time on Biological Effectiveness and

Tumor Control Probability in Proton Therapy. Int J Radiat Oncol Biol Phys 2019;105(1):222-229.

21. Brenner DJ, Hlatky LR, Hahnfeldt PJ. The Linear-quadratic model and most other common radiobiological models result in similar predictions of time-dose relationships. Radiat Res 1998;150:83-91.

22. Brenner DJ. The linear-quadratic model is an appropriate methodology for determining isoeffective doses at large doses per fraction. Semin Radiat Oncol 2008;18:234-239.

23. Hyland WB, McMahon SJ, Butterworth KT. Investigation into the radiobiological consequences of pre-treatment verification imaging with megavoltage X-rays in radiotherapy. Br J Radiol 2014;87:20130781

24. Bewes JM, Suchowerska N, Cartwright L. Optimization of temporal dose modulation: Comparison of theory and experiment. Med Phys 2012;39:3181-3188.

25. Sato T, Iwamoto Y, Hashimoto S. Features of particle and heavy ion transport code system (PHITS) version 3.02. J Nucl Sci Technol 2018;55:684-690.

26. Sato T, Kase Y, Watanabe R. Biological dose estimation for charged-particle therapy using an improved PHITS code coupled with a microdosimetric kinetic model. Radiat Res 2009;171:107-17.

27. Sato T, Furusawa Y. Cell survival fraction estimation based on the probability densities of domain and cell nucleus specific energies using improved micorodosimetric kinetic models. Radiat Res 2012;178:341-56.

28. Sato T, Hamada N. Model Assembly for estimating cell surviving fraction for both targeted and nontargeted effects based on microdosimetric probability densities. Plos One 2014;9:e114056.

29. Okamoto H, Kanai T, Kase Y. Relation between lineal energy distribution and relative biological effectiveness for photon beams according to the microdosimetric

kinetic model. J Radiat Res 2011;52:75-81.

30. King RB, Hyland WB, Cole AJ. An in vitro study of the radiobiological effects of flattening filter free radiotherapy treatments. Phys Med Biol 2013;58:83-94.

31. Okamoto H, Kohno T, Kanai T. Microdosimetric study on influence of low energy photons on relative biological effectiveness under therapeutic conditions using 6 MV linac. Med Phys 2011;38:4714-4722.

32. Faught JT, Balter PA, Johnson JL. An FMEA evaluation of intensity modulated radiation therapy dose delivery failures at tolerance criteria levels. Med Phys 2017;44: 5575-5583.

33. Dang TM, Peters MJ, Hickey B. Efficacy of flattening -filter-free beam in stereotactic body radiation therapy planning and treatment: A systematic review with meta-analysis. J Med Imaging Radiat Oncol 2017; 61:379-387.

34. Polo A. High-dose-rate and pulsed-dose-rate brachytherapy for oral cavity cancer and oropharynx cancer. J Contemp Brachytherapy 2009; 1:216-223.

Figure Legends

Fig. 1. Diagram of the mMK model, taking into consideration the interruption time of photon beams.

Fig. 2. Irradiation geometry for the Monte Carlo calculations with 6 MV photon beams. The radius of the domain was set to 0.5 μm in the 3-cm-wide measurement region with the water-equivalent phantom.

Fig. 3. The microdosimetric energy distributions yD as a function of y-yd(y) for 6 MV photon beams at a depth of 10 cm in a water-equivalent phantom **(a)**. The relationship between the depth (which was 3 cm from the measurement point in the water equivalent phantom) and the dose-mean lineal energy yD for the 6 MV photon beams **(b)**.

Fig. 4. The effect of the interruption time on the SF for 6 MV photon beams with two-field **(a)** and four-field **(b)** irradiation for the various interruption times.

Fig. 5. The effect of the interruption time on the RBE with two-field **(a)** and four-field **(b)** irradiation for the various interruption times.

Fig. 6. The effect of prolonging the interruption time (1 to 60 min) on the RBE when two-field irradiation was used.

Fig. 7. The effect of RBE as a function of the cell-specific repair rate (a + c) with $\tau = 1$ min **(a)** and $\tau = 10$ min **(b)** using two-field irradiation.

Figures

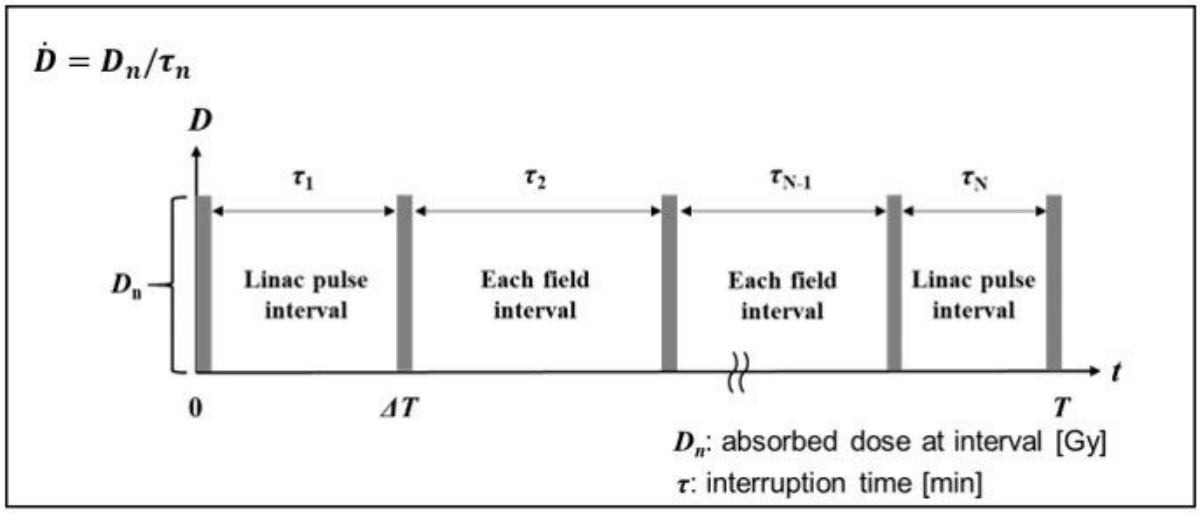

Figure 1

Diagram of the mMK model, taking into consideration the interruption time of photon beams.

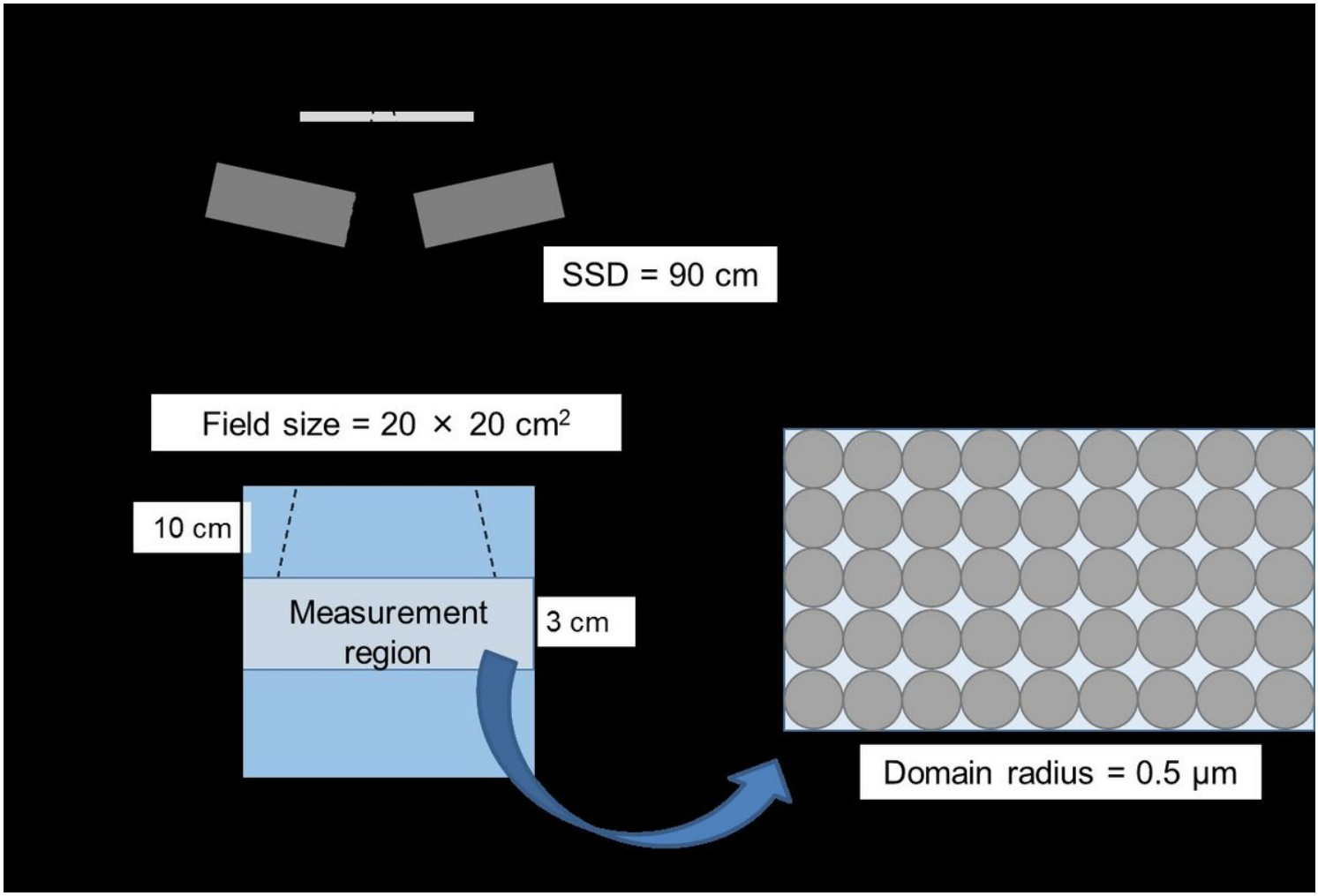

Figure 2

Irradiation geometry for the Monte Carlo calculations with 6 MV photon beams. The radius of the domain was set to 0.5 μm in the 3-cm-wide measurement region with the water-equivalent phantom.

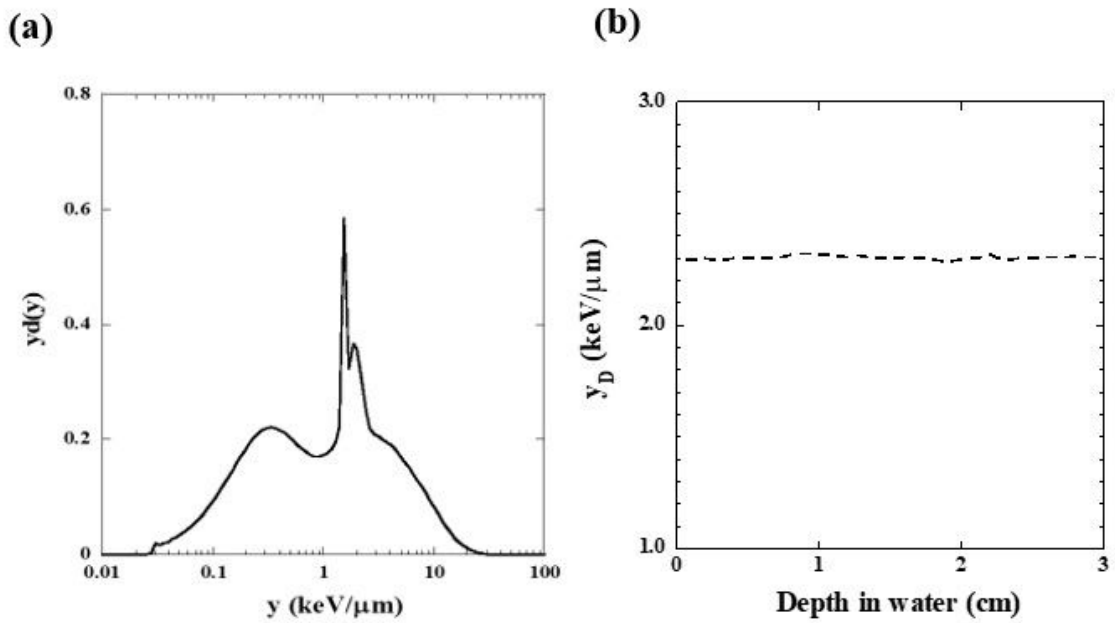

Figure 3

The microdosimetric energy distributions yD as a function of y-yd(y) for 6 MV photon beams at a depth of 10 cm in a water-equivalent phantom (a). The relationship between the depth (which was 3 cm from the measurement point in the water equivalent phantom) and the dose-mean lineal energy yD for the 6 MV photon beams (b).

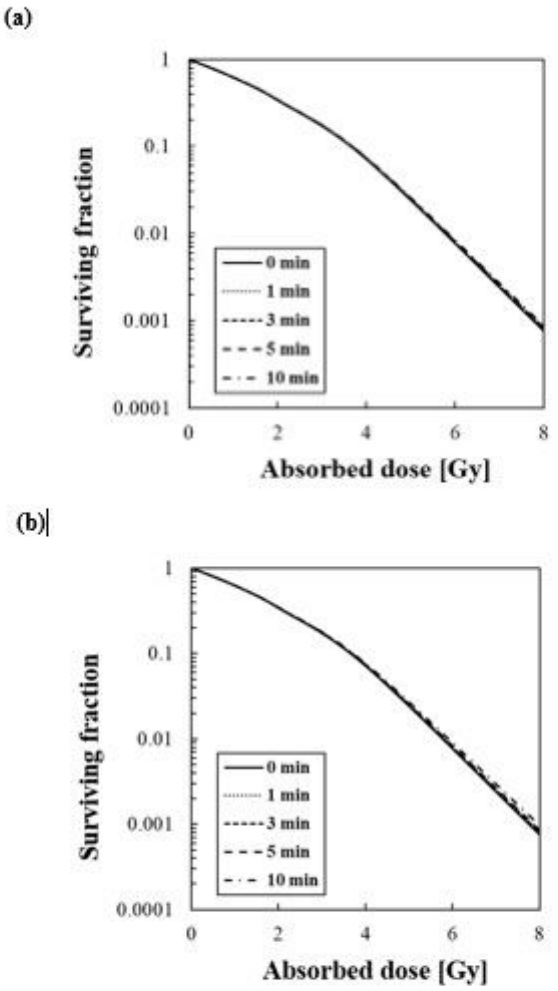

Fig. 4.

Figure 4

The effect of the interruption time on the SF for 6 MV photon beams with two-field (a) and four-field (b) irradiation for the various interruption times.

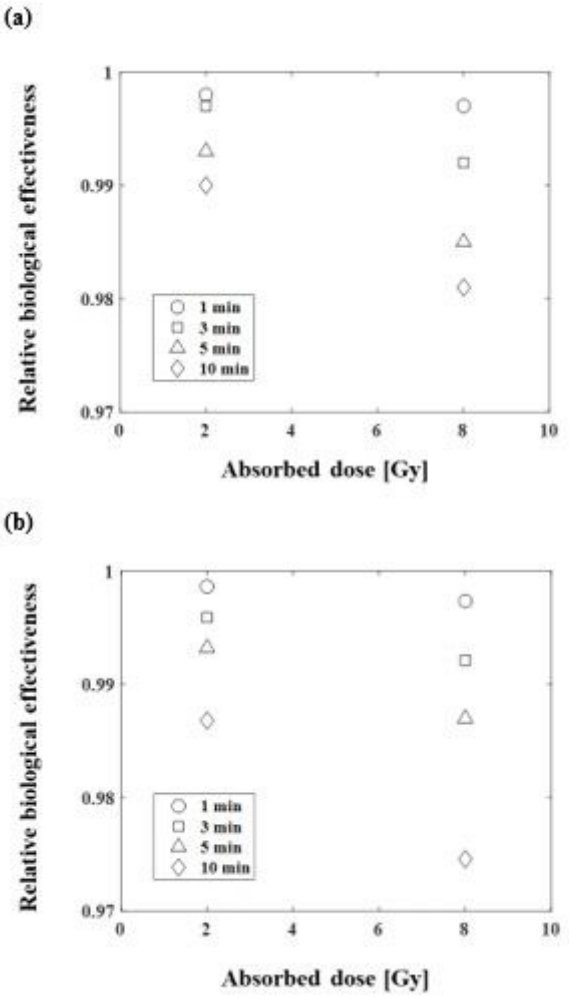

Figure 5

The effect of the interruption time on the RBE with two-field (a) and four-field (b) irradiation for the various interruption times.

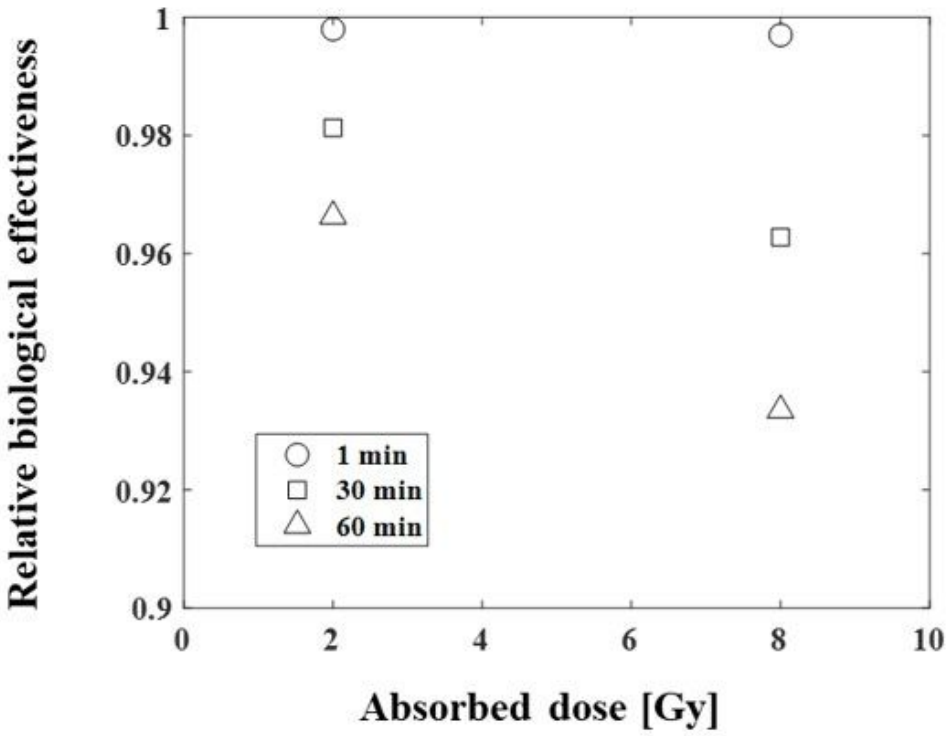

Figure 6

The effect of prolonging the interruption time (1 to 60 min) on the RBE when two-field irradiation was used.

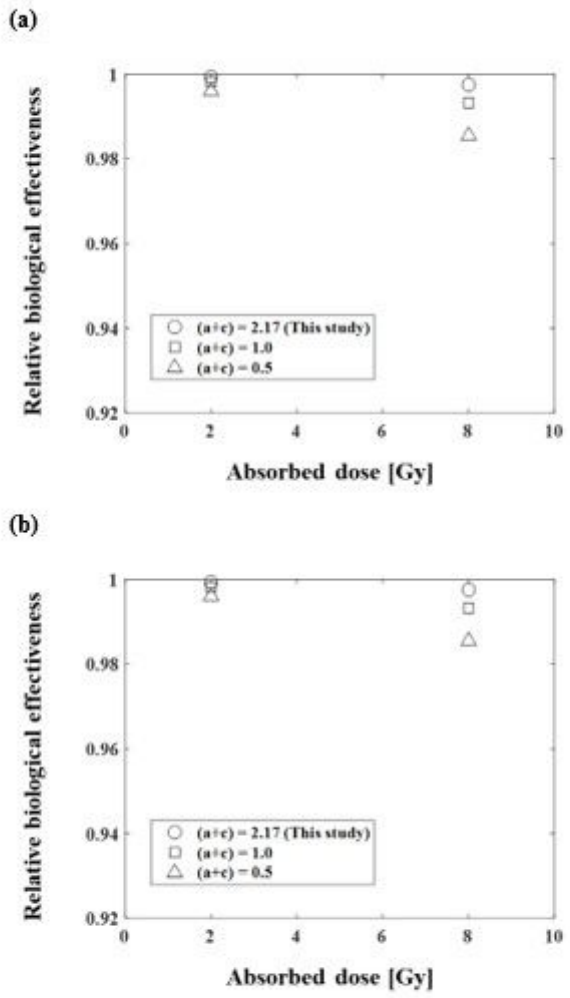

Fig. 7.

Figure 7

The effect of RBE as a function of the cell-specific repair rate (a + c) with τ = 1 min (a) and τ = 10 min (b) using two-field irradiation.